



Analysis of the process and factors influencing microbial phosphine production

Yimin Fan¹ · Xiaojun Niu^{2,3} · Dongqing Zhang²

Received: 20 December 2022 / Accepted: 24 April 2023 / Published online: 27 May 2023
© The Author(s), under exclusive licence to Springer-Verlag GmbH Germany, part of Springer Nature 2023

Abstract

The process of phosphine production by phosphate-reducing bacteria *Pseudoscherichia* sp. SFM4 has been well studied. Phosphine originates from the biochemical stage of functional bacteria that synthesize pyruvate. Stirring the aggregated bacterial mass and supplying pure hydrogen could lead to an increase of 40 and 44% phosphine production, respectively. Phosphine was produced when bacterial cells agglomerated in the reactor. Extracellular polymeric substances secreted on microbial aggregates promoted the formation of phosphine due to the presence of groups containing phosphorus element. Phosphorus metabolism gene and phosphorus source analysis implied that functional bacteria used anabolic organic phosphorus, especially containing carbon-phosphorus bonds, as a source with [H] as electron donor to produce phosphine.

Keywords Phosphine · Extracellular polymeric substances · Hydrogen · Organic phosphorus

Introduction

Phosphine, a reactive and highly toxic reducing gas, is a significant constituent of global phosphorus biogeochemical cycle (Niu et al. 2013). Phosphine, or matrix-bound phosphine (MBP), is extensively distributed in the environment, such as in the sediment (Feng et al. 2008; Hou et al. 2009; Song et al. 2011), urban air (Ji-Ang et al. 1999), anaerobic pond (Roels et al. 2002), landfill (Roels and Verstraete 2004), and even polar region (Zhu et al. 2006). Phosphine accumulated in lake sediments can be released into the water, resulting in enhanced eutrophication (Geng et al. 2005). Phosphine in the atmosphere is oxidized to

phosphate and rained out, which results in the accumulation of phosphorus in the soil. Furthermore, hydroxyl radicals that aid in reducing greenhouse gases are absorbed by the phosphine in the atmosphere, which indirectly aggravated global warming (Glindemann et al. 2003). In addition, phosphine has been regarded as a biomarker (Greaves et al. 2020; Sousa-Silva et al. 2020). Therefore, exploring the mechanisms involved in phosphine formation is crucial.

Although the detection of phosphine in aquatic environments has been extensively investigated, the mechanisms of phosphine production are still up for debate, especially whether phosphine is produced as a product of bacterial metabolism or by the attack of acid-bacterial metabolites on environmental phosphide. The potential biological pathways of phosphine production have been proposed before (Bains et al. 2019a; Niu et al. 2013). Furthermore, anaerobic digestion processes exhibit high potential of increasing the phosphine yield (Fan et al. 2020b). However, how this affects the metabolic pathways during phosphine formation remains unclear.

Microbial phosphine production often occurs in organisms that form aggregates in culture and are not in isolated single cells. Extracellular polymeric substances (EPS), organic polymers mainly derived from cell secretion and autolysis during biological processes (Flemming and Wingender 2001), play an essential role in mass transfer, flocculation, precipitation, and the formation of microbial aggregates

Responsible Editor: Philippe Garrigues

✉ Xiaojun Niu
xjniu@scut.edu.cn

¹ School of Civil Engineering and Architecture, Taizhou University, Taizhou 318000, People's Republic of China

² Guangdong Provincial Key Laboratory of Petrochemical Pollution Processes and Control, School of Environmental Science and Engineering, Guangdong University of Petrochemical Technology, Maoming 525000, People's Republic of China

³ School of Environment and Energy, South China University of Technology, Guangzhou 510006, People's Republic of China

(Adav et al. 2008; Huang et al. 2017). In general, EPS are divided into tightly bound EPS (TB-EPS) and loosely bound EPS (LB-EPS), depending on what is wrapped outside the cell (Li and Yang 2007). EPS can be degraded into small molecules by extracellular enzymes that provide substrate and energy for microbial growth (Zhang et al. 2015). However, to date, little information is available about the effect of EPS on phosphine production by microorganisms.

A previous study revealed that a single phosphine-producing strain exhibited the ability for hydrogen production (Fan et al. 2021). The biological pathways of hydrogen production include the decarboxylation of pyruvate in the glycolysis process and the redox balance of coenzyme I (nicotinamide adenine dinucleotide (NADH/NAD⁺)) (Yong et al. 2002). Assuming that [H] is used as an electron donor for phosphine production, as shown in Eq. 8 $[H] + H^+ + H_2PO_4^- \rightarrow PH_3 + 4H_2O$. The NADH related to hydrogen production also promoted the production of phosphine (Fan et al. 2020a). The microbial absorption of inorganic phosphorus in the aquatic environment is accomplished by phosphorus transporters, such as inorganic phosphate transport A (PitA) and phosphate-specific transport S (PstS) (Gao and Stock 2013). However, to date, no direct experimental evidence supports that hydrogen promotes phosphine production. Further studies are therefore indispensable to explore the relationship between microbial hydrogen and phosphine production.

In this study, microbial phosphine production was analyzed based on the composition analysis of substrate dehydrogenation by-products. Then, the effect of microbial aggregates and hydrogen on phosphine production was evaluated. Finally, the roles of EPS and different phosphorus sources in phosphine production were explored.

Materials and methods

The acquisition of phosphine producing strain

The functional bacteria growing on the culture medium were initially isolated. DNA from the functional bacteria was extracted using the rapid DNA extraction kit (KG203-02, Tiangen Biotech Co., Ltd., Beijing), following according to the manufacturer's instructions. Bacterial 16S ribosomal DNA fragments were amplified using polymerase chain reaction (PCR) using the universal bacterial primer set with forward primer 338 F (50-ACTCCTACGGGAGGCAGC A-30) and reverse primer 806 R (50-GGACTACHVGGG TWTCTAAT-30) in the V3–V4 hypervariable region. PCR product quality was validated using electrophoresis on 2% agarose gel. The amplified production was sequenced by Sangon Biotech Co., Ltd. (Shanghai, China). The phylogenetic tree was constructed using MEGA 7, as listed

in Supplementary information Fig. S1. It was evidenced that functional bacteria were associated with Proteobacteria (phylum), *γ-Proteobacteria* (class), *Enterobacteriales* (order), *Enterobacteriaceae* (family), and *Pseudodescherichia* (genus). The functional bacterium was named *Pseudodescherichia* sp. SFM4 (OP765491), and the sequence was submitted to the NCBI. The phosphine production performance of this strain has been reported (Fan et al. 2021).

Phosphine production in an anaerobic sequencing batch reactor

A vacuum flask (Shuniu, Sichuan Shubo Co., Ltd., Sichuan) of 1500 mL was set up as a reactor for microbial to phosphine production. The modified culture medium used for phosphine production was prepared as follows: 250 mg/L glucose, 20 mg/L KH₂PO₄, 40 mg/L K₂HPO₄·3H₂O, 38 mg/L NH₄Cl, 50 mg/L ascorbic acid, and 1 mL/L trace elements. The stock solution was prepared as follows: 1.5 g/L NTA, 0.3 g/L MgSO₄·7H₂O, 0.1 g/L FeSO₄·7H₂O, 1 g/L NaCl, 0.1 g/L CoCl₂·6H₂O, 0.1 g/L CaCl₂, 0.1 g/L ZnSO₄·7H₂O, 0.01 g/L CuSO₄·5H₂O, 0.01 g/L KAl(SO₄)₂·12H₂O, 0.01 g/L H₃BO₃, and 0.1 g/L Na₂MoO₄·2H₂O. The pH was adjusted to 8.5 with 1 mol/L NaOH. The prepared medium was deoxygenated with nitrogen for 15 min and then autoclaved at 121 °C for 20 min. The reactor was inoculated with phosphine-producing bacteria 20% (v/v) in the initial stages. The batch mode was adopted in reactor; each reaction cycle was set at 80 h, drainage and feed were performed at the last 15 min of each cycle. The temperature was kept at 35 °C. The samples were collected at an interval of every 4 h.

Microbial aggregates and hydrogen function analysis

Four reactors were operated in parallel for 4 h, 12 h, 32 h, and 64 h. After the reaction, 900 mL of supernatant was discarded and 100 mL of residual was retained. The characteristics of microbial aggregates were analyzed by measuring volatile solid (VS) concentrations (Orhororo et al. 2017). To further assess the influence of microbial aggregates on phosphine production, experiments were carried out in 250 mL conical flasks at different stirring rates (i.e., 0, 300, 500, 700, and 900 rpm). The conical flask was sealed by a rubber stopper with short glass tubes. The gas was collected by a polyester gas collecting bag (Hede Technologies Co., Ltd., Dalian) connected to the glass tube. The concentration of phosphine production was measured every 24 h. Additionally, evaluating the effect of hydrogen on production phosphine production, two assays were designed as follows: 100 mL of pure hydrogen and nitrogen (control) were introduced into conical flasks 1 and 2, respectively.

Molecular biology analysis

At the time points of 4 and 32 h, 50 mL of residuals were collected. After centrifugation (TGL-16 M, Xiangyi centrifuge instrument Co., Ltd., Changsha), genomic DNA was extracted from the residuals using rapid DNA extraction kit (see “[The acquisition of phosphine-producing strain](#)” section). The DNA concentration was determined using a NanoDrop (NanoDrop Technologies Inc., Wilmington, DE, USA). The *pitA* and *pstT* genes of functional bacteria were amplified using PCR with the synthesized primers, as shown in Table S1. The PCR was performed at 95 °C for 60 s; 40 three-segment cycles of 95 °C for 5 s; 60 °C, 15 s; 72 °C, 34 s; final extension at 72 °C, 10 min. The PCR products were pooled and purified using PCR purification kit (DP214-02, Tiangen Biotech Co., Ltd., Beijing). The resulting libraries were sequenced using the Illumina MiSeq platform (Majorbio Bio-Pharm Technology Co., Ltd., China).

Four phosphorus-transporter genes were selected for quantitative amplification using real-time PCR (qPCR). Gene name, primer pairs, and amplified band size is shown in Table S1. Total RNA was extracted from the residuals using an RNA extraction kit (DP430, Tiangen Biotech Co., Ltd., Beijing), following the manufacturer’s instructions, and 2 µL of it was reverse transcribed at 42 °C using the M5 First Strand cDNA Synthesis Kit (ZR108-1, Zoman Biotechnology Co., Ltd., Beijing). Single reaction was performed for each cDNA along with the serial dilution using the PerfectStart™ Green qPCR SuperMix (AQ602-11, TransGen Biotech Co., Ltd., Beijing). An aliquot of 20 µL containing 2 µL of cDNA and 0.8 µL of each primer was prepared for each reaction. The qPCR performed on a fluorescence SLAN48-P qPCR system (Hongshi Medical Technology Co., Ltd., Shanghai); the cycling processes were as follows: 1 cycle of denaturation at 94 °C for 30 s; followed by 40 three-segment cycles of amplification consisting of 95 °C for 5 s; 50–63 °C, 15 min; 72 °C, 34 s.

The effect of phosphorus conversion on phosphine producing

In order to analyze the phosphorus conversion related to phosphine production by functional microbes, the anaerobic incubation assay was operated using different types of organophosphorus. An aliquot of 10 mg of phosphorus was added as either trimethylphosphine or phosphoenolpyruvate (PEP). The control experiment used phosphate as the phosphorus source. The headspace gas was collected with 100 mL syringes every 24 h. The concentration of phosphine was determined after 32 h of reaction.

The effect of EPS on phosphine producing

Both TB-EPS and LB-EPS were extracted from each microbial aggregate collected at 4 and 32 h using the modified method of thermal extraction (Yang and Li 2009), in which 50 mL of microbial aggregates were centrifuged at 15,000 g for 15 min at 4 °C. The precipitate was resuspended by adding 50 mL of preheated 0.05% (*w/v*) NaCl (50 °C). After centrifugation, the organic matter in the suspension was regarded as LB-EPS. As for the extraction of TB-EPS, the precipitate was resuspended by adding preheated NaCl (60 °C) using a water bath at 400 rpm for 30 min. To investigate the functional intracellular or extracellular bacteria related to phosphine production, bio-reactor and non-bioreactor with EPS introduction were operated using 250-mL conical flasks with rubber stoppers.

Analytical methods

Phosphine was enriched in Al₂O₃/Na₂SO₄ capillary chromatographic columns with dimensions of 1 m×0.53 mm×3.0 µm (Chase Scientific Instruments Co., Ltd., China), coupled with two successive capillary cryotrap (Beijing Ai Feibo Co., Ltd., China). The concentration of enriched phosphine was determined using gas chromatography (Agilent 7820A, USA), equipped with flame ionization detector (FID) and HP-5 columns (19091 J-413 30 m×0.32 mm×0.25 µm, Agilent, USA). H₂ and CO₂ were measured using gas chromatography (Agilent 7820A, USA), equipped with thermal conductivity detector (TCD), and packed column (TDX-01, ATEO, China). The concentrations of pyruvic acid, acetic acid, and lactic acid were detected using high-performance liquid chromatography (HPLC) (Shimadzu LC-20A, Japan), coupled with AQ-C18 column (30 mm×2.1 mm×3.0 µm, Aupos, Germany). pH was measured using a pH meter (pb-10, Sartorius, Germany). The alteration in microbial morphology was observed using scanning electron microscopy (SEM) (LEO1530VP, Zeiss, Germany). The concentration of VS was determined following the method described by Orhorhoro (Orhorhoro et al. 2017). The levels of total phosphorus and phosphate were measured according to Standard Methods (Federation and Association 2005). The chemical composition of the EPS at different phases was determined using three-dimensional fluorescence excitation-emission matrix (FEEM) spectrophotometer (HITACHI F7000, China) and Fourier transform infrared (FTIR) scanning (VERTEX 70, Bruker, Germany).

Results

The processes of microbial phosphine production

Figure 1a illustrates the variation in phosphine produced by microbes over time using glucose as substrate. The

phosphine produced by the microorganism was observed only in a specific period of 12–40 h, and the maximum phosphine concentration was 75 mg/m^3 observed at 32 h. This finding indicated that there must be a predominant pathway for phosphine generation via bacterial metabolism. The changes in pyruvate concentration with time are presented in Fig. 1b. After 4 h, 30 mg/L pyruvate and 29 mg/L lactic acid (Fig. 1c) were rapidly produced during decomposition of glucose, resulting in a sharp decrease in pH from 8.3 to 5.0. During the phase of 4–12 h, the concentration of acetic acid and lactic acid reduced from 30 to 12 mg/L. As such, the reaction period of 0–12 h was considered a catabolism process, in which the glucose was decomposed into pyruvate and further broken down into simple compounds such as acetic acid and lactic acid. However, the microbial catabolism in this period was not accompanied by the production of phosphine (Fig. 1a). As

illustrated in Fig. 1c, during the interval of 12–32 h, the concentration of acetic acid and lactic acid reduced from 38 and 37 to 10 and 12 mg/L, respectively. Meanwhile, the concentration of pyruvate increased from 10 to 40 mg/L (Fig. 1b), coupled with a significant increase in phosphine production.

During the period of 4–12 h, the hydrogen concentration increased from 0 to 0.7 mg/L and pyruvate was decomposed; in contrast, during the interval of 12–32 h, a substantial rise in the hydrogen concentration was observed from 0.7 to 2.5 mg/L. Coenzyme I produce hydrogen to regulate redox balance has been demonstrated (Tanisho and Ishiwata 1995), and large amounts of hydrogen were derived from the redox balance of coenzyme I. This stage was accompanied by an increase in the concentration of phosphine. Hydrogen production observed in this phase implied that more energy and reduced power were generated compared to those in other stage.

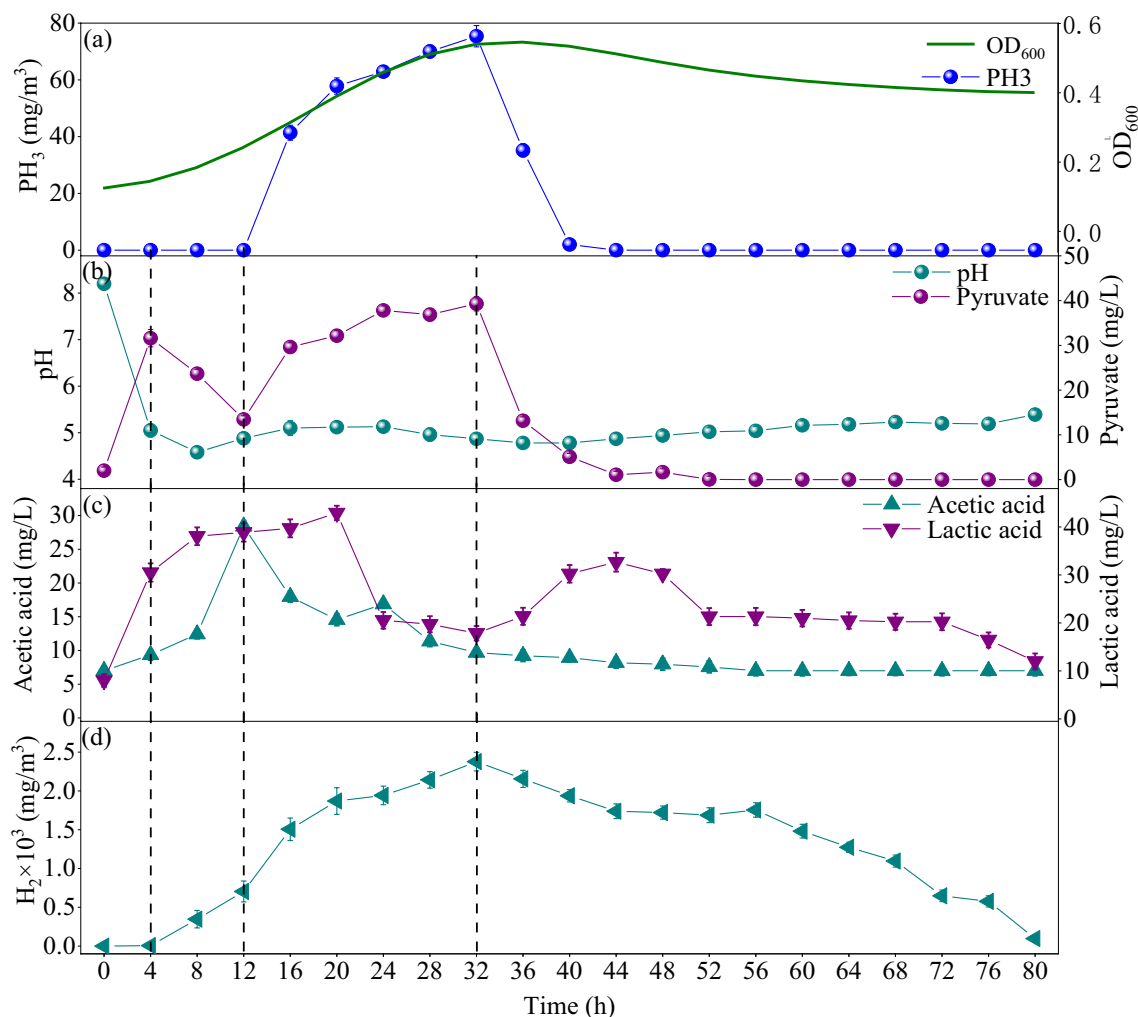


Fig. 1 Biological oxidation of bacteria using glucose as substrate to produce **a** phosphine; **b** pyruvate; **c** acetic acid and lactic acid; **d** H₂

Influence of microbial aggregates and hydrogen

The bacterial accumulation overtime during the biological phosphine production in the reactors is shown in Supplementary information Fig. S2. Morphological changes in microbial polymer during cell aggregation and dehydration were observed using SEM, as shown in Fig. 2. After 4 h of reaction, no microbial aggregates were observed due to the function bacteria in the lag phase. After 12 h, the bacterial cells started to aggregate and agglomerate, reaching the maximum precipitation at 32 h. Particularly, the level of EPS was significantly enhanced at 32 h. VS was used to characterize the concentration of microbial aggregates. After 12 h, the microbes continued to aggregate and settle at the bottom of the reactor. The highest VS concentration was 0.03 mg/L at 32 h. The VS increase rate was 0.0004 mg/L/h during 4–12 h and VS 0.000245 mg/L/h during 12–32 h. After 64 h, due to the rupture of the cells, the disintegration of the flocs occurred, and the broken flocs settled at the bottom, resulting in a decrease in the VS. This finding implied that phosphine production (12–32 h, 0–75 mg/m³) required a certain density and stable colloidal structure of the microbes.

To further assess the effect of microbial aggregation on the production of phosphine, the aggregated bacterial mass was resuspended by stirring. As presented in Fig. 3a, the maximum phosphine concentration of 250 mg/m³ was observed when the stirring speed was 700 rpm at 24 h, which was three times greater compared to that in the unstirred reactor. However, the concentration of endogenous hydrogen decreased with the increase in the stirring speed (Fig. 3b). The maximum concentration of hydrogen in the control (2 mg/L) was higher than that in the treatment with 700 rpm stirring speed (0.3 mg/L). Similarly, previous study also indicated that the performance of anaerobes, converting organic wastes into hydrogen, decreases at the stirring speed exceeding 120 rpm (Chou et al. 2008). Moreover, at stirring speed of 700 rpm, compared with the unstirred, the concentration of phosphine generated in the treatment with hydrogen feeding, increased from 180 to 260 mg/m³ (Fig. 3c). When the cultures have a large excess of [H] to dispose of (e.g., lactate to pyruvate conversion or under H₂ atmosphere) and are well dispersed (extensive protein EPS or by stirring), so that cross-feeding is inefficient, hydrogenase is saturated, and PH₃ is produced.

Role of EPS in the formation of phosphine

The aggregation and agglomeration of microbes is observed in phosphine production, which correlates to the production of extracellular polymers. As shown in Fig. 4, protein (PN) and polysaccharides (PS) were the main components of EPS, and the concentration of PN (11 mg/L) was five times that of PS at 32 h (2 mg/L). Compared with PS, extracellular

enzymes and PN bind to each other easily through electrostatic attraction and multivalent cations, facilitating the structural stability of microbial aggregates (Zhu et al. 2009). Furthermore, compared with TB-EPS (PN), LB-EPS (PN) increased significantly from 3 to 7 mg/L within 4–32 h, implying that LB-EPS (PN) played a significant role in the process of microbial aggregation, rather than TB-EPS (PN).

The chemical composition of EPS in different phases was determined using 3D-FEEM. Five peaks were identified by the fluorescence spectrum, representing tyrosine-like protein (EX/EM 200–250/200–330) in region I; tryptophan-like protein (EX/EM 200–250/330–380), region II; fulvic acid-like organics (EX/EM 200–250/380–500), region III; soluble microbial by-product (250–280/200–380), region IV; and humic acid-like organics (250–400/380–500) in region V (Guo et al. 2014). As shown in Fig. 5, the strongest fluorescence intensity was observed at the excitation/emission 275/330 nm, implying that the predominant chemical composition of EPS was soluble microbial by-product. The fluorescence intensities of LB-EPS at various phases were apparently stronger compared to those of TB-EPS. Phosphine production is maximum at 32 h, which follows the highest fluorescence intensity of LB-EPS and TB-EPS. This finding indicates that with vigorous growth and rapid propagation, microorganisms exhibited strong catalytic activity and produced more metabolic by-products at 32 h. Previous finding (Fig. 2c) indicated that functional bacteria were necessary for phosphine production, suggesting that strong microbial activity was conducive to its production.

As illustrated in Fig. 5e, the results of FTIR analysis showed that the chemical compositions of EPS primarily consisted of polysaccharides and proteins. The predominant infrared bands observed at 1080 and 1647 cm⁻¹ were associated with the C–OH stretching of polysaccharides and stretching vibration of C=O and C–N (amide I) of proteins, respectively. Infrared spectrum band located at 1418 cm⁻¹ was assigned to COO-symmetrical stretching, while the band at 2929 cm⁻¹ represented CH₂⁻ antisymmetric stretching. Pyruvate and acetic acid, having functional groups C=O, COOH, C–OH, and CH₂⁻, respectively, can promote phosphine production. Infrared spectrum bands at 1239 and 1140 cm⁻¹ were related to PO²⁻ and PO⁻, respectively. These functional groups were derived from lipids and nucleic acids contained in EPS. Therefore, EPS could promote phosphine production by providing functional groups responsible for the synthesis of phosphine-related substances.

Regarding the phosphorus source analysis

The functional bacterial strain added in the assays was *Pseudoscherichia* sp. SFM4. As presented in Fig. S4, the abundance of *Pseudoscherichia* spp. at 4 and 32 h exceeded 95%, although

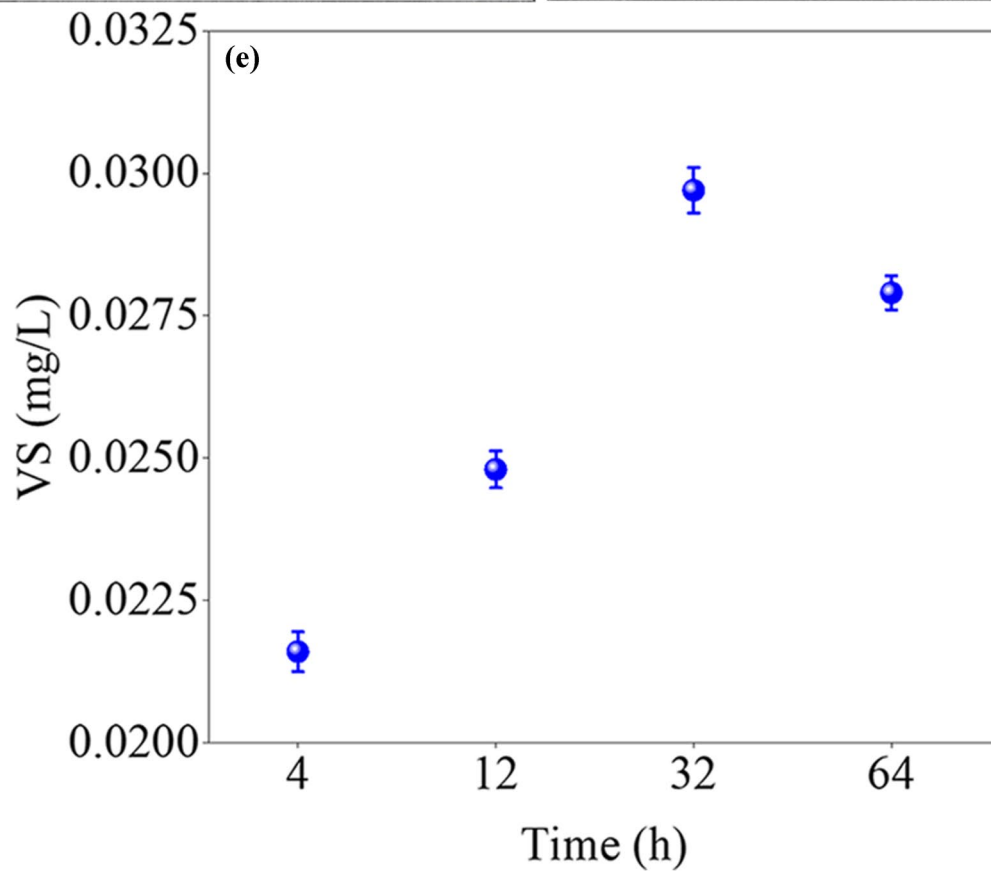
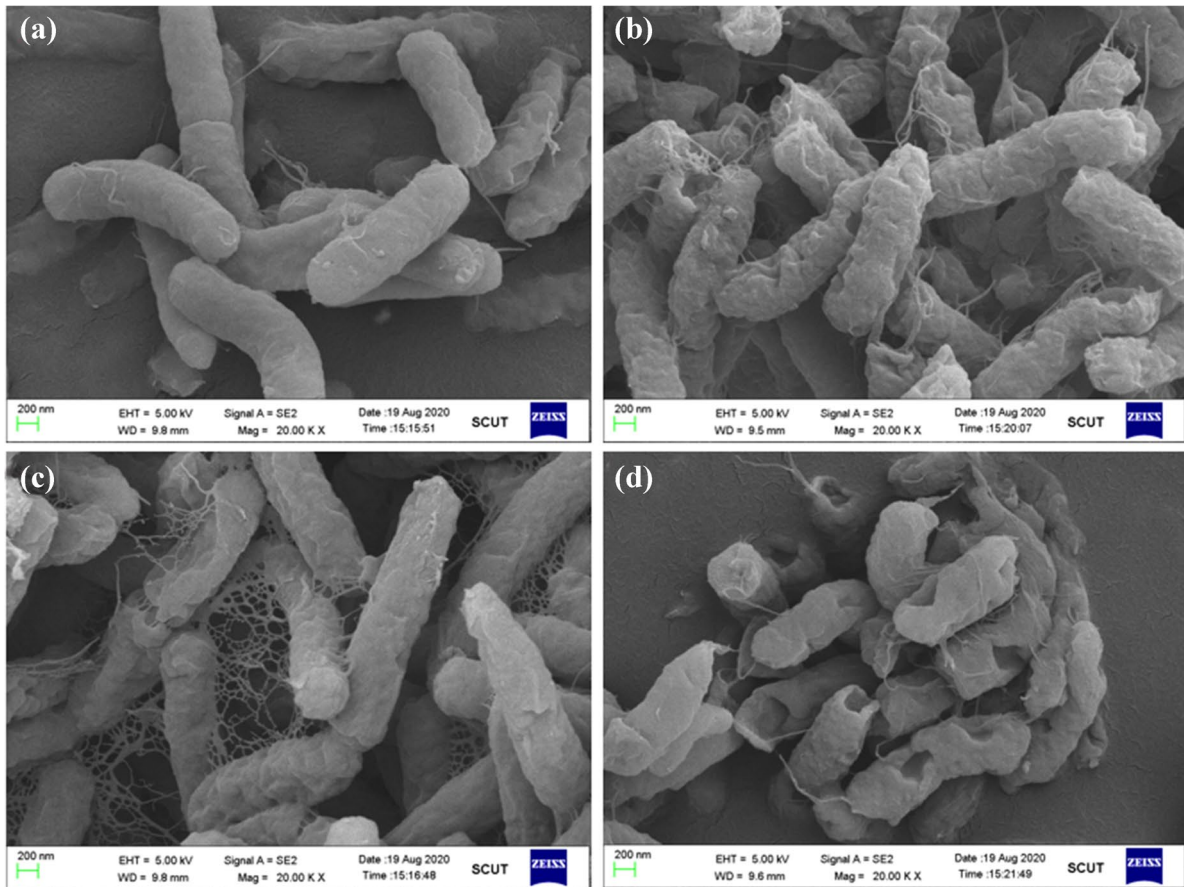


Fig. 2 Scanning electron microscopy (SEM) spectra of bacterial clusters in the period of **a** 4 h; **b** 12 h; **c** 32 h; **d** 64 h; **e** the analysis of volatile solids

there were other bacteria involved in the biological process for phosphine production, it was evidenced that *Pseudodescherichia* sp. SFM4 were the dominant bacterial species responsible for phosphine production. Several studies have revealed that phosphine production was positively related to the phosphatase produced by microorganisms (Liu et al. 2008). Thus, to determine the expression of phosphatase, i.e., *phoN* and *phoD*, qPCR analysis was carried out. As shown in Fig. 6a, the results indicated that *phoN* and *phoD* were significantly up-regulated from 4 to 32 h. Organic phosphorus in anaerobic digestion was decomposed by phosphatase, which was used by microbes as the source of phosphorus to produce phosphine. The addition of organic phosphorus containing carbon-phosphorus (C-P) bonds promoted the production of phosphine (Han et al. 2002). Microorganisms can transport phosphate through the phosphate-specific transport system (Pst) and the phosphate transport system (Pit) (Bergkemper et al. 2016). As illustrated in Fig. 6a, the expression of phosphorus transporter genes *pitA* and *pstS* were downregulated at 32 h compared with those at 4 h. This finding implied that although the functional bacteria reduced the demand for phosphate from 4 to 32 h, the yield of phosphine substantially increased in this period.

As shown in Fig. 6b, the addition of different phosphides, i.e., trimethylphosphorus (with C–P bonds) and phosphoenolpyruvate (without C–P bonds). Highest phosphine concentration of 160 mg/m³ was observed in the reactor after

treatment with trimethylphosphorus. In general, organic phosphorus, especially organic phosphorus containing carbon-phosphorus (C–P) bonds, was more conducive to the production of phosphine compared to inorganic phosphorus. The introduction of phosphonoacetic acid containing C–P bonds into the fermentation reactor with paddy soil led to an increase in the concentration of phosphine by 100 times (Han et al. 2002). As illustrated in Fig. 6c, inorganic phosphorus enters the cell through the phosphorus transport system, which synthesizes organophosphorus. The initial step in the biosynthesis of the phosphonates (C–P), virtually common to all known pathways, involves a reversible intramolecular rearrangement of the intermediary metabolite PEP to phosphonopyruvate by the enzyme phosphoenolpyruvate phosphomutase (PepM) (Chin et al. 2016).

Discussion

Microbial phosphine production pathway

In this study, the metabolic pathways of microbial phosphine production were analyzed using isolated functional bacteria. Glucose undergoes biological oxidation to produce simple molecules for phosphine production during anaerobic digestion associated with the production of energy (Fan et al. 2021). We suggest that intermediate product pyruvate is decomposed to acetic acid and lactic acid between 4 and 12 h. Between 12 and 32 h, pyruvate concentration rises again, which coincides with increased phosphine production.

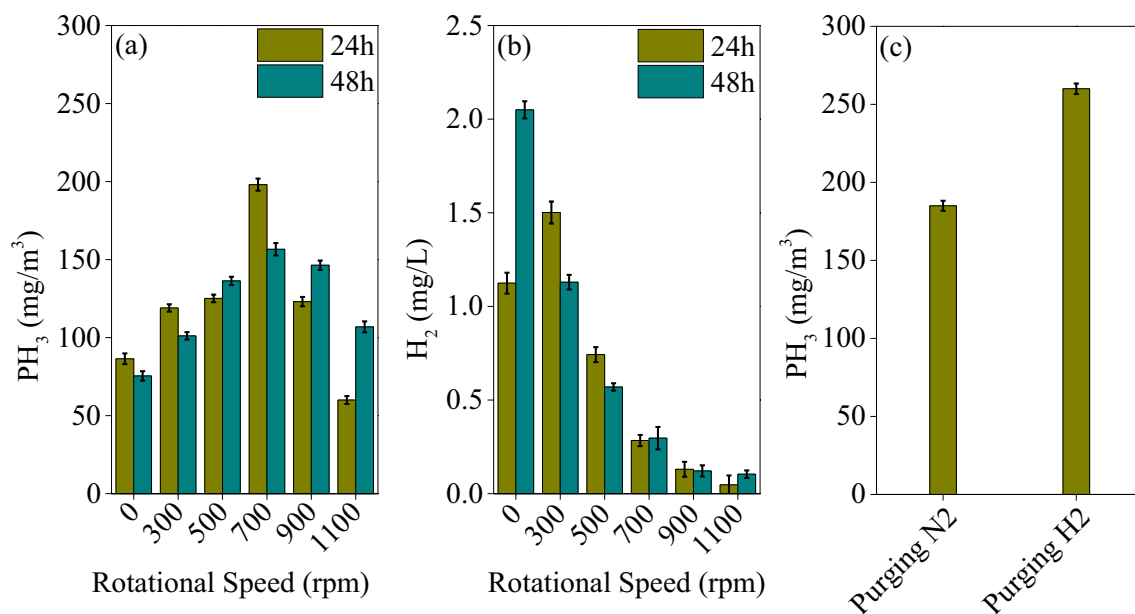


Fig. 3 The effect of stirring on the production performance of **a** phosphine, **b** hydrogen, and **c** phosphine in reactor with the introduction of nitrogen and hydrogen

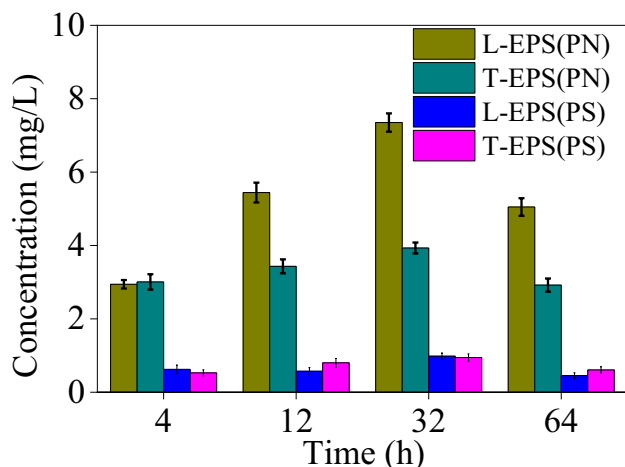


Fig. 4 The concentration of polysaccharide and protein of EPS extracted in different time periods

The biosynthesis of phosphonates (C–P) to phosphonopyruvate by the PepM involves a reversible intramolecular rearrangement of the intermediate metabolite PEP (Chin et al. 2016). The experimental results also show that phosphate as a source of phosphorus contributes more to the production of phosphine than inorganic phosphorus (Fig. 6b). In this study, phosphine production was accompanied by the biosynthesis of pyruvate, indicating that phosphine originated from biochemical stage of functional bacteria which synthesize pyruvate.

Analysis of electron donor

It is been well documented that for hydrogen production, decarboxylation of pyruvate occurs during bacterial metabolism (Ren et al. 1997), and regulation of redox balance through coenzyme I (NADH/NAD⁺) is necessary (Tanisho and Ishiwata 1995). The reducing power

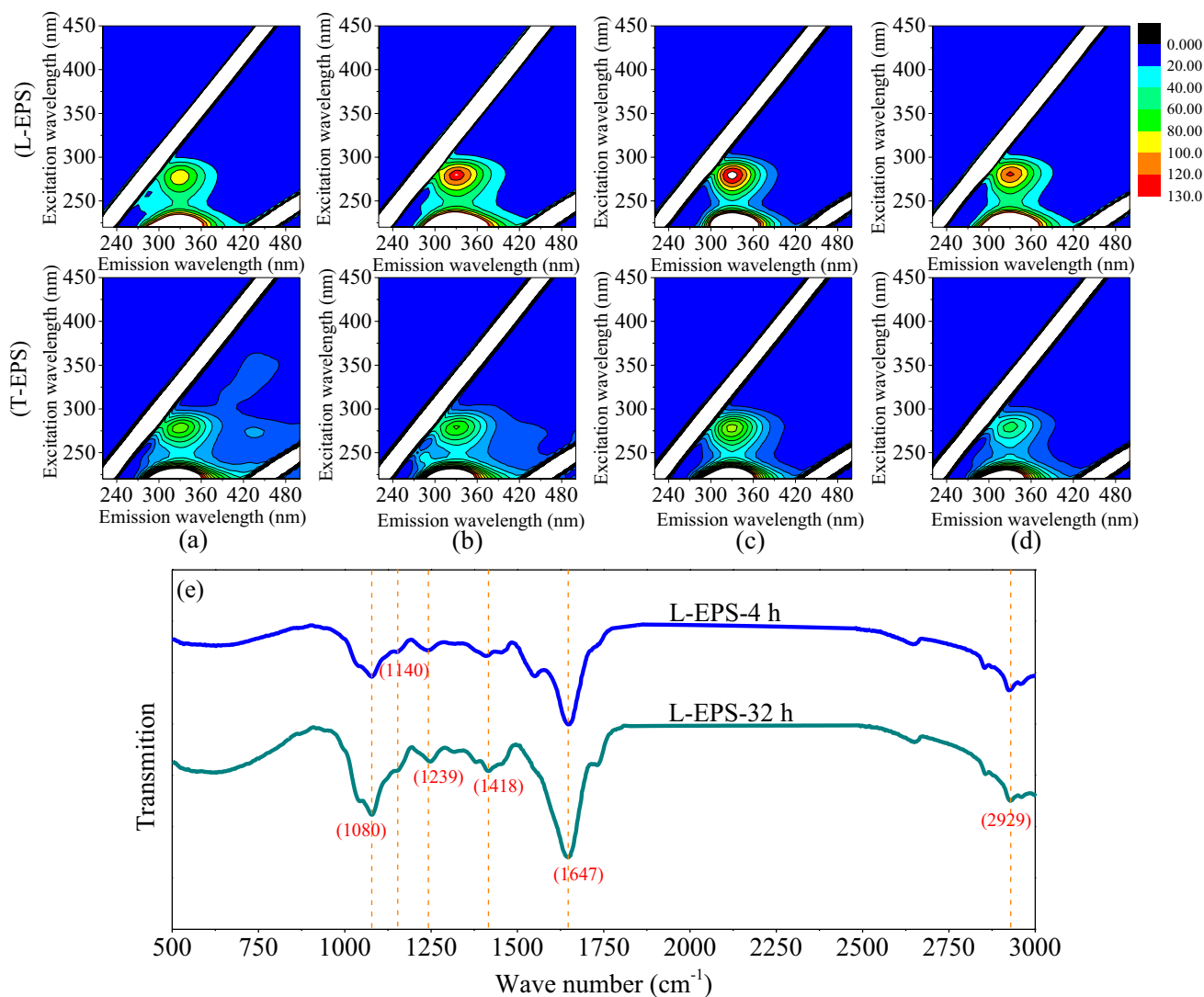


Fig. 5 Three-dimensional fluorescence analysis of L-EPS and T-EPS at **a** 4 h; **b** 12 h; **c** 32 h; **d** 64 h; **e** FTIR spectra of the L-EPS at 4 and 32 h

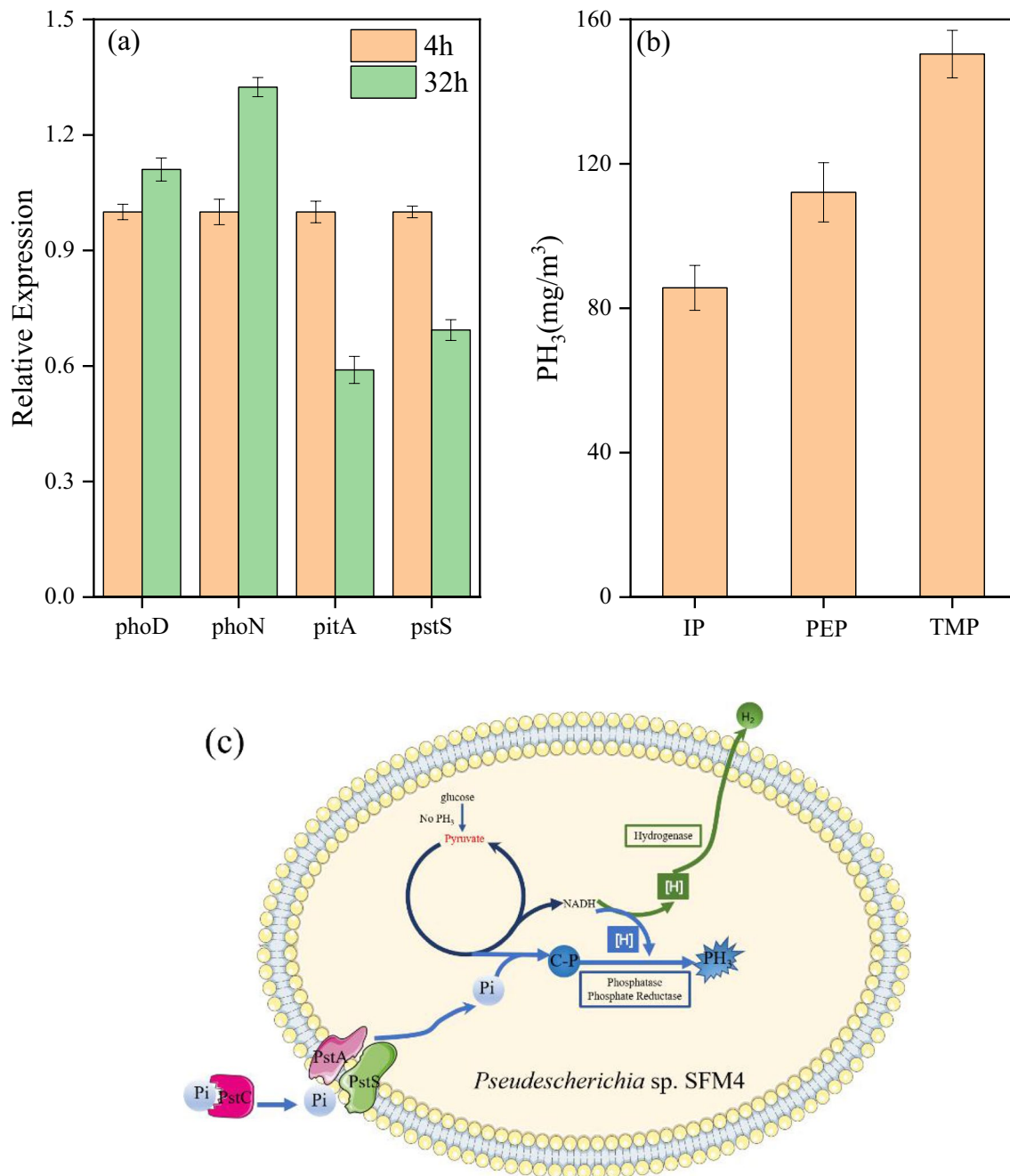


Fig. 6 Analysis of **a** genes related to phosphorus metabolism based on q-PCR, **b** PH₃ with the addition of different phosphides, and **c** mechanism of phosphine production (TMP, trimethylphosphorus; PEP, phosphoenolpyruvate; IP, inorganic-phosphorus)

of NADH plays an essential role in electron transport, maintaining cell growth, energy metabolism, as well as cell protection (Gray and Gest 1965). The intracellular redox carrier NADH, a more powerful reducing agent compared to hydrogen, is most likely to be involved in phosphine formation (Bains et al. 2019b). During cell metabolism, excessive reducing power of NADH is generated and released through the formation of molecular hydrogen. Hydrogen was not detected in 0–4 h, indicating

that few NADH-reducing power was generated during glucose decomposition subject to pyruvate formation, so phosphine was not detected. These findings suggest that phosphine production is enhanced when pyruvic acids are formed due to the generation of more NADH. Phosphine production is strongly coupled to pyruvate, low pH, and high hydrogen production. It is unlikely that H₂ acts as an electron donor to make PH₃ because that reaction is thermodynamically unfavorable (when hypophosphite is

used as a source of phosphorus, microorganisms produce the highest concentration of phosphine but the lowest concentration of hydrogen; Supplementary information Fig. S5). However, hydrogenase is reversible, so culturing in a hydrogen atmosphere will reduce the net flux of [H] through hydrogenase and hence increase the level of [H] as NADH in the cell. The hypothesis is that PH₃ is produced when hydrogenase cannot get rid of enough [H] from the cell to balance the cell's internal redox potential. The P–C and hypophosphite promote PH₃ formation, and PH₃ formation is dependent on saturation with [H].

Analysis of phosphorus conversion for phosphine

Microorganisms aggregate during phosphine production. Phosphine might be serving as a signaling molecule to promote the aggregation of bacteria. The protein concentration in both TB-EPS and VS increased, while the content of polysaccharides decreased in the reactor with the addition of phosphine (Supplementary Information Fig. S3). The produced phosphine may act as a signaling molecule released by microbial quorum sensing (Sousa-Silva et al. 2020), which can be considered an autoinducer released by microorganisms into the environment that can freely diffuse between cells in order to stimulate the expression of bacteria-related genes in response to the physiological behavior (Fuqua et al. 1994). Similarly, Ren et al. (2013) reported that the signaling molecules were secreted by the aerobic granular sludge, facilitating the aggregation of suspended *Escherichia coli*. Microorganisms generate organophosphorus (e.g., phosphoenolpyruvate) during the synthesis of pyruvate. Phosphorus metabolism gene and phosphorus source analysis reinforced the fact that phosphine production by functional bacteria was derived from the decomposition of organophosphorus with C-P bonds coupled with phosphatase. Many studies have reported a positive correlation between phosphine production and microbial alkaline phosphatase activity (An et al. 2018; Fan et al. 2020a; Liu et al. 2021).

Conclusion

Here, the metabolic pathways of microbial phosphine production were analyzed using isolated functional bacteria. When the cultures have a large excess of [H] to dispose of (e.g., lactate to pyruvate conversion or under H₂ atmosphere) and are well dispersed (extensive protein EPS or by stirring) so that cross-feeding is inefficient, hydrogenase is saturated, and PH₃ is produced. Phosphorus metabolism gene and phosphorus source analysis reinforced the fact that phosphine production by functional bacteria was derived from the decomposition of organophosphate coupled with phosphatase.

Supplementary Information The online version contains supplementary material available at <https://doi.org/10.1007/s11356-023-27293-7>.

Author contribution Yimin Fan: conceptualization, methodology, software, and investigation. Xiaojun Niu: validation, formal analysis, visualization, software, and data curation. Dongqing Zhang: validation, formal analysis, visualization, and writing—reviewing and editing.

Funding This work was supported by the National Natural Science Foundation of China (no. 42177369), the National Key Research and Development Program of China (no. 2019YFA0210400), the Science and Technology Planning Project of Maoming, China (no. 2019S002), and the Fundamental Research Funds for the Central Universities, SCUT (no. 2020ZYGXZR105).

Data availability Not applicable.

Declarations

Ethical approval Not applicable.

Consent to participate Not applicable.

Consent for publication Not applicable.

Competing interest The authors declare no competing interest.

References

- Adav SS, Lee DJ, Tay JH (2008) Extracellular polymeric substances and structural stability of aerobic granule. *Water Res* 42(6–7):1644–1650
- An S, Niu X, Chen W, Sheng H, Lai S, Yang Z, Gu X, Zhou S (2018) Mechanism of matrix-bound phosphine production in response to atmospheric elevated CO₂ in paddy soils. *Environ Pollut* 239:253–260
- Bains W, Petkowski JJ, Sousa-Silva C, Seager S (2019a) New environmental model for thermodynamic ecology of biological phosphine production. *Sci Total Environ* 658:521–536
- Bains W, Petkowski JJ, Sousa-Silva C, Seager S (2019b) Trivalent phosphorus and phosphines as components of biochemistry in anoxic environments. *Astrobiology* 19(7):885–902
- Bergkemper F, Kublik S, Lang F, Krüger J, Vestergaard G, Schloter M, Schulz S (2016) Novel oligonucleotide primers reveal a high diversity of microbes which drive phosphorous turnover in soil. *J Microbiol Methods* 125:91–97
- Chin JP, McGrath JW, Quinn JP (2016) Microbial transformations in phosphonate biosynthesis and catabolism, and their importance in nutrient cycling. *Curr Opin Chem Biol* 31:50–57
- Chou C-H, Wang C-W, Huang C-C, Lay J-J (2008) Pilot study of the influence of stirring and pH on anaerobes converting high-solid organic wastes to hydrogen. *Int J Hydrogen Energy* 33(5):1550–1558
- Fan Y, Lv M, Niu X, Ma J, Song Q (2020a) Evidence and mechanism of biological formation of phosphine from the perspective of the tricarboxylic acid cycle. *Int Biodeterior Biodegrad* 146:104791
- Fan Y, Lv M, Niu X, Ma J, Zhang D (2020b) The key step of gaseous phosphorus release in anaerobic digestion. *Process Saf Environ Protect* 137:238–245
- Fan Y, Niu X, Zhang D, Lin Z, Fu M, Zhou S (2021) Analysis of the characteristics of phosphine production by anaerobic digestion based on microbial community dynamics, metabolic pathways, and isolation of the phosphate-reducing strain. *Chemosphere* 262:128213

- Federation WE, Association A (2005) Standard methods for the examination of water and wastewater. American Public Health Association, Washington
- Feng Z, Song X, Yu Z (2008) Seasonal and spatial distribution of matrix-bound phosphine and its relationship with the environment in the Changjiang River Estuary, China. *Mar Pollut Bull* 56(9):1630–1636
- Flemming HC, Wingender J (2001) Relevance of microbial extracellular polymeric substances (EPSs) - part I: structural and ecological aspects. *Water Sci Technol* 43(6):1–8
- Fuqua W, Claiborne W, Stephen C (1994) Quorum sensing in bacteria: the LuxR-LuxI family of cell density-responsive transcriptional. *J Bacteriol* 176(2):269–275
- Gao R, Stock AM (2013) Evolutionary tuning of protein expression levels of a positively autoregulated two-component system. *PLoS Genet* 9(10):e1003927
- Geng J, Jin X, Wang Q, Niu X, Wang X, Edwards M, Glindemann D (2005) Matrix bound phosphine formation and depletion in eutrophic lake sediment fermentation—simulation of different environmental factors. *Anaerobe* 11(5):273–279
- Glindemann D, Edwards M, Kusch P (2003) Phosphine gas in the upper troposphere. *Atmos Environ* 37(18):2429–2433
- Gray CT, Gest H (1965) Biological formation of molecular hydrogen: a "hydrogen valve" facilitates regulation of anaerobic energy metabolism in many microorganisms. *Science* 148(3667):186–192
- Greaves JS, Richards AM, Bains W, Rimmer PB, Sagawa H, Clements DL et al (2020) Phosphine gas in the cloud decks of Venus. *Nat Astron* 5(7):655–664
- Guo L, Lu M, Li Q, Zhang J, Zong Y, She Z (2014) Three-dimensional fluorescence excitation–emission matrix (EEM) spectroscopy with regional integration analysis for assessing waste sludge hydrolysis treated with multi-enzyme and thermophilic bacteria. *Biores Technol* 171:22–28
- Han SH, Zhuang YH, Zhang HX, Wang ZJ, Yang JZ (2002) Phosphine and methane generation by the addition of organic compounds containing carbon–phosphorus bonds into incubated soil. *Chemosphere* 49(6):651–657
- Hou LJ, Chen H, Yang Y, Jiang JM, Lin X, Liu M (2009) Occurrence of matrix-bound phosphine in intertidal sediments of the Yangtze Estuary. *Chemosphere* 76(8):1114–1119
- Huang J, Qi F, Zeng G, Shi L, Li X (2017) Repeating recovery and reuse of SDS micelles from MEUF retentate containing Cd²⁺ by acidification UF. *Colloid Surface A* 520:361–368
- Ji-Ang L, Yahui CHZ, Kusch P, Eismann F, Glindemann D (1999) Phosphine in the urban air of Beijing and its possible sources. *Water Air Soil Pollut* 116(3):597–604
- Li XY, Yang SF (2007) Influence of loosely bound extracellular polymeric substances (EPS) on the flocculation, sedimentation and dewaterability of activated sludge. *Water Res* 41(5):1022–1030
- Liu Z, Jia S, Wang B, Mang T, Liu S (2008) Preliminary investigation on the role of microorganisms in the production of phosphine. *J Environ Sci* 20(7):885–890
- Liu WM, Xu W, Qin ML, Wang WG, Shen B, Xu L (2021) Direct electrooxidation synthesis of nickel hypophosphite and its application in electroless nickel plating. *Int J Electrochem Sc* 19(9):210943
- Niu X, Mi L, Li Y, Wei A, Yang Z, Wu J, Zhang D, Song X (2013) Physiological and biochemical responses of rice seeds to phosphine exposure during germination. *Chemosphere* 93(10):2239–2244
- Orhorhoro EK, Ebunilo PO, Sadjere GE (2017) Experimental determination of effect of total solid (TS) and volatile solid (VS) on biogas yield. *Am J Modern Energy* 3(6):131–135
- Ren N, Wang B, Huang JC (1997) Ethanol-type fermentation from carbohydrate in high rate acidogenic reactor. *Biotechnol Bioeng* 54(5):428–433
- Ren T-T, Li X-Y, Yu H-Q (2013) Effect of N-acyl-homoserine lactones-like molecules from aerobic granules on biofilm formation by *Escherichia coli* K12. *Biores Technol* 129:655–658
- Roels J, Verstraete W (2004) Occurrence and origin of phosphine in landfill gas. *Sci Total Environ* 327(1):185–196
- Roels J, Van Langenhove H, Verstraete W (2002) Determination of phosphine in biogas and sludge at ppt-levels with gas chromatography-thermionic specific detection. *J Chromatogr A* 952(1–2):229–237
- Song X, Morrison RJ, Feng Z, Liu D, Harrison JJ, Yu Z (2011) Matrix-bound phosphine in sediments from Lake Illawarra, New South Wales, Australia. *Mar Pollut Bull* 62(8):1744–1750
- Sousa-Silva C, Seager S, Ranjan S, Petkowski JJ, Zhan Z, Hu R, Bains W (2020) Phosphine as a biosignature gas in exoplanet atmospheres. *Astrobiology* 20(2):235–268
- Tanisho S, Ishiwata Y (1995) Continuous hydrogen production from molasses by fermentation using urethane foam as a support of flocks. *Int J Hydrogen Energy* 20(7):541–545
- Yang S-F, Li X-Y (2009) Influences of extracellular polymeric substances (EPS) on the characteristics of activated sludge under non-steady-state conditions. *Process Biochem* 44(1):91–96
- Yong W, Nanqi R, Yujiao S (2002) Analysis on the mechanism and capacity of two types of hydrogen production-ethanol fermentation and butyric acid fermentation. *Acta Energetica Solaris Sinica* 23:366–373
- Zhang P, Guo J-S, Shen Y, Yan P, Chen Y-P, Wang H, Yang J-X, Fang F, Li C (2015) Microbial communities, extracellular proteomics and polysaccharides: a comparative investigation on biofilm and suspended sludge. *Biores Technol* 190:21–28
- Zhu R, Sun L, Kong D, Geng J, Wang N, Wang Q, Wang X (2006) Matrix-bound phosphine in Antarctic biosphere. *Chemosphere* 64(8):1429–1435
- Zhu P, Long G, Ni J, Tong M (2009) Deposition kinetics of extracellular polymeric substances (EPS) on silica in monovalent and divalent salts. *Environ Sci Technol* 43(15):5699–5704

Publisher's note Springer Nature remains neutral with regard to jurisdictional claims in published maps and institutional affiliations.

Springer Nature or its licensor (e.g. a society or other partner) holds exclusive rights to this article under a publishing agreement with the author(s) or other rightsholder(s); author self-archiving of the accepted manuscript version of this article is solely governed by the terms of such publishing agreement and applicable law.